Supporting information for

Effect of Polymer Branching and Average Molar Mass on the Formation, Stabilization and Thermoresponsive properties of Gold Nanohybrids Stabilized by Poly(N-isopropylacrylamide).

Hong Hanh Nguyen,[a] Annie Brûlet,[b] Dominique Goudounèche,[c] Pascale Saint-Aguet,[d] Nancy Lauth-de Viguerie*[a] and Jean-Daniel Marty*[a]

[a] IMRCP, Université de Toulouse, CNRS UMR 5623, 31062 Toulouse Cedex 09, France

[b] Laboratoire Léon Brillouin, UMR12 CEA-CNRS, CEA Saclay, F-91191 GIF/Yvette, France

[c] CMEAB, IFR-BMT, Université de Toulouse, 133 route de Narbonne, 31062 Toulouse, France.

[d] Technopolym, ICT, FR 2599, Université de Toulouse, 118 route de Narbonne, 31062 Toulouse, France.

Contents

A. Synthesis and characterization of polymers

A.1. Evaluation of grafting efficiency

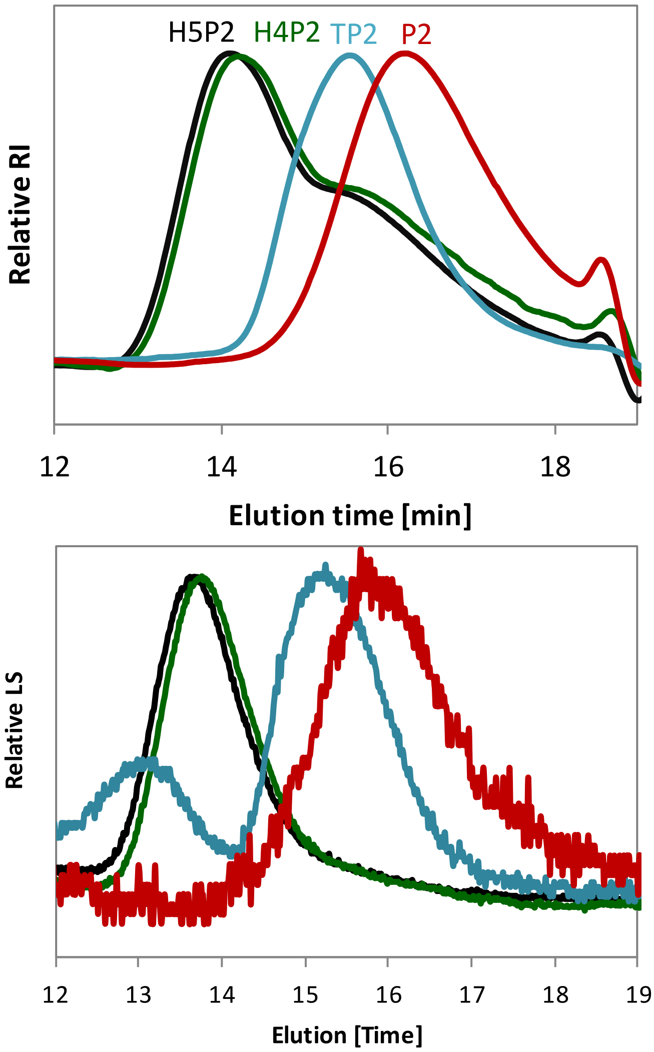

Figure SI 1. SEC chromatograms of P2, TP2, H4P2 and H5P2 in DMF (LiCl, 1g.L^{-1}) at 40°C (flow rate, 1 mL·min^{1}): refractive index (top) and light scattering responses (bottom).

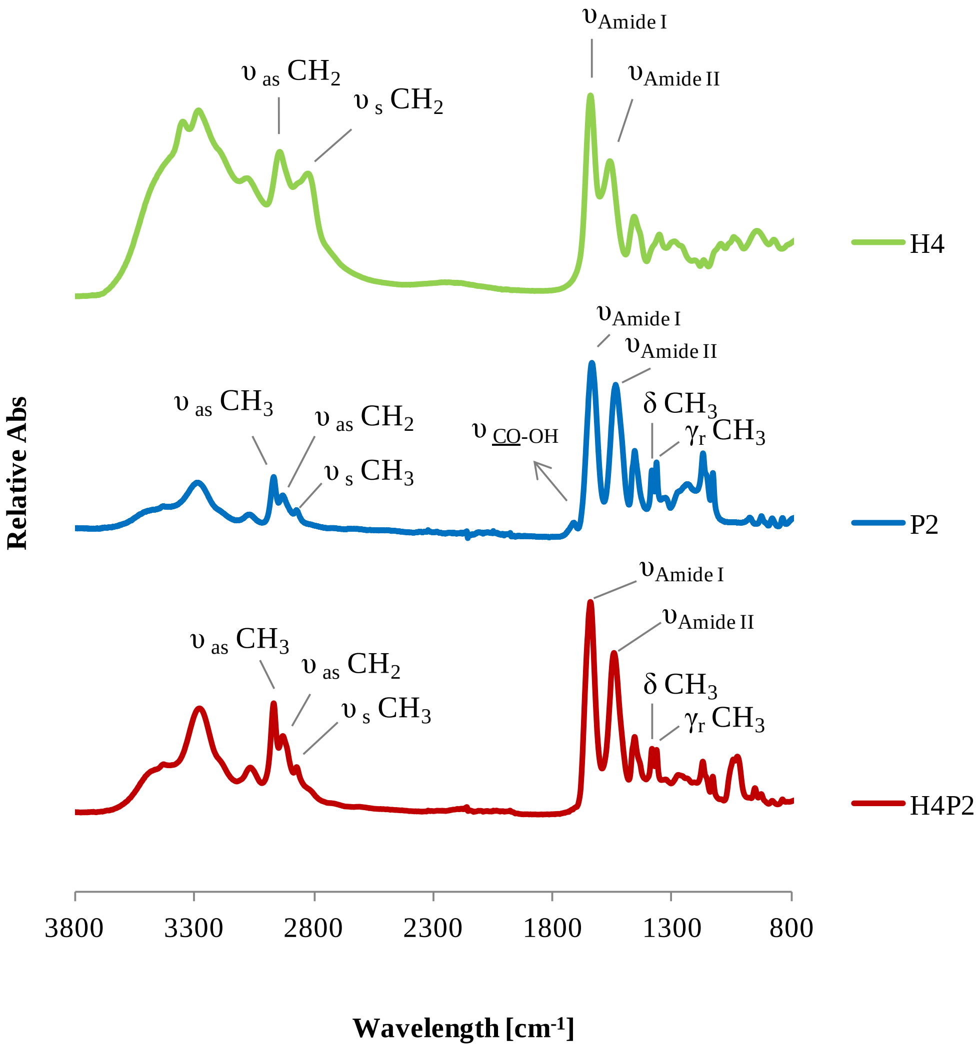

Figure SI 2. ATR-FTIR spectra of H4, P2 and H4P2.

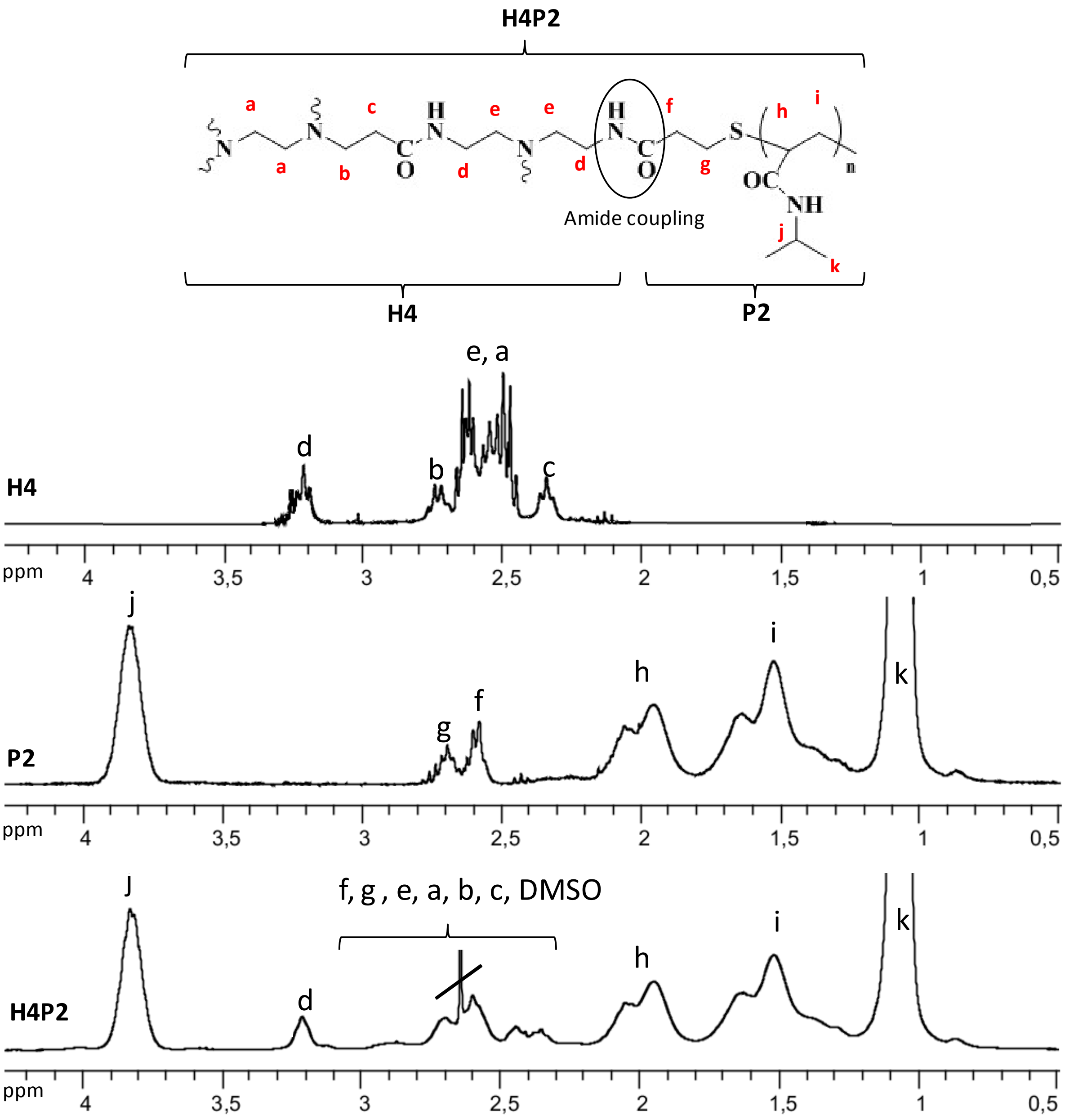

Figure SI 3. ^{1}H NMR spectra of H4, P2 and H4P2 (300Hz, 298K, D$_2$O).

Characterization of polymers by ^{1}H NMR and by IR:

TP5 ------------------------

^{1}H NMR (D$_2$O, 300Hz): 1.06 (CO-NH-CH-*CH*$_3$ PNIPAM), 1.51 (CH-*CH*$_2$ PNIPAM), 1.93 (*CH*-CH$_2$ main chain PNIPAM), 2.35 (N-CH$_2$-*CH*$_2$-NH-CO), 2.45 (N-*CH*$_2$-CH$_2$-NH-CO), 2.60 (CO-*CH*$_2$-CH$_2$-S PNIPAM), 2.70 (CO-CH$_2$-*CH*$_2$-S PNIPAM), 3.83 (CO-NH-*CH*-CH$_3$ PNIPAM)
IR: $\bar{\nu}$ = 3426, 3288, 3075, 2972, 2933, 2876, 1634, 1534, 1457, 1386, 1366, 1266, 1172, 1130, 970, 926, 877, 838 cm^{-1}

TP7 ------------------------

^{1}H NMR (D$_2$O, 300Hz): 1.03 (CO-NH-CH-*CH*$_3$ PNIPAM), 1.90 (*CH*-CH$_2$ main chain PNIPAM), 1.51 (CH-*CH*$_2$ PNIPAM), 2.36 (N-CH$_2$-*CH*$_2$-NH-CO), 2.45 (N-*CH*$_2$-CH$_2$-NH-CO), 2.60 (CO-*CH*$_2$-CH$_2$-S PNIPAM), 2.71 (CO-CH$_2$-*CH*$_2$-S PNIPAM), 3.83 (CO-NH-*CH*-CH$_3$ PNIPAM)
IR: $\bar{\nu}$ = 3433, 3288, 3076, 2972, 2934, 2875, 1538, 1458, 1386, 1366, 1262, 1172, 1131, 1026, 927, 882, 838 cm^{-1}

H4P5 ----------------------

^{1}H NMR (D_2O, 500Hz): 1.0 (CO-NH-CH-*CH_3* PNIPAM), 1.43 (CH-*CH_2* PNIPAM), 1.86 (*CH*-CH_2 main chain PNIPAM), 2.27 (CO-*CH_2*-CH_2-S PNIPAM), 2.37 (N-CH_2-*CH_2*-CO), 2.45 (N-*CH_2*-*CH_2*-N), 2.51 (CO-NH-CH_2-*CH_2*), 2.55 (CO-CH_2-*CH_2*-S PNIPAM), 2.63(N-*CH_2*-CH_2-CO), 3.23 (CO-NH-*CH_2*-CH_2),: 3.75 (CO-NH-*CH*-CH_3 PNIPAM)

^{13}C NMR (D_2O, 500Hz): 53.59 (N-*CH_2*-*CH_2*-N), 51.1 (N-*CH_2*-CH_2-CO), 35.09 (N-CH_2-*CH_2*-CO), 36.51 (CO-NH-*CH_2*-CH_2), 52.0 (CO-NH-CH_2-*CH_2*), 37.04 (CO-*CH_2*-CH_2-S), 27.80 (CO-CH_2-*CH_2*-S), 42.7 (*CH*-CH_2 main chain PNIPAM), 35.01 (CH-*CH_2*), 41.8 (CO-NH-*CH*-CH_3),: 21.7. (CO-NH-CH-*CH_3*), 174 (*CO*-NH).

IR: $\bar{\nu}$ = 3434, 3283, 3076, 2971, 2933, 2875, 1639, 1583, 1386, 1366, 1270, 1172, 1130, 1025, 973, 927, 882, 839 cm^{-1}

H4P7 ----------------------

^{1}H NMR (D_2O, 500Hz): 1.0 (CO-NH-CH-*CH_3* PNIPAM 1.44 (CH-*CH_2* PNIPAM),), 1.87 (*CH*-CH_2 main chain PNIPAM), 2.28 (CO-*CH_2*-CH_2-S PNIPAM), 2.37 (N-CH_2-*CH_2*-CO), 2.45 (N-*CH_2*-*CH_2*-N), 2.53 (CO-NH-CH_2-*CH_2*), 2.55 (CO-CH_2-*CH_2*-S PNIPAM), 2.63(N-*CH_2*-CH_2-CO), 3.23 (CO-NH-*CH_2*-CH_2),: 3.75 (CO-NH-*CH*-CH_3 PNIPAM)

^{13}C NMR (D_2O, 500Hz): 53.61 (N-*CH_2*-*CH_2*-N), 51.1 (N-*CH_2*-CH_2-CO), 35.08 (N-CH_2-*CH_2*-CO), 36.51 (CO-NH-*CH_2*-CH_2), 52.01 (CO-NH-CH_2-*CH_2*), 37.05 (CO-*CH_2*-CH_2-S), 27.80 (CO-CH_2-*CH_2*-S), 42.7 (*CH*-CH_2 main chain PNIPAM), 35.01 (CH-*CH_2*), 41.8 (CO-NH-*CH*-CH_3),: 21.7. (CO-NH-CH-*CH_3*), 174 (*CO*-NH).

IR: $\bar{\nu}$ = 3434, 3288, 3073, 2972, 2933, 2857, 1641, 1542, 1458, 1386, 1366, 1268, 1172, 1130, 1026, 975, 927, 882, 838 cm^{-1}

H5P2 ----------------------

^{1}H NMR (D_2O, 500Hz): 1.01 (CO-NH-CH-*CH_3* PNIPAM 1.44 (CH-*CH_2* PNIPAM),), 1.88 (*CH*-CH_2 main chain PNIPAM), 2.27 (CO-*CH_2*-CH_2-S PNIPAM), 2.37 (N-CH_2-*CH_2*-CO), 2.45 (N-*CH_2*-*CH_2*-N), 2.53 (CO-NH-CH_2-*CH_2*), 2.55 (CO-CH_2-*CH_2*-S PNIPAM), 2.63(N-*CH_2*-CH_2-CO), 3.23 (CO-NH-*CH_2*-CH_2),: 3.75 (CO-NH-*CH*-CH_3 PNIPAM)

^{13}C NMR (D_2O, 500Hz): 53.6 (N-*CH_2*-*CH_2*-N), 51.11 (N-*CH_2*-CH_2-CO), 35.10 (N-CH_2-*CH_2*-CO), 36.50 (CO-NH-*CH_2*-CH_2), 52.01 (CO-NH-CH_2-*CH_2*), 37.05 (CO-*CH_2*-CH_2-S), 27.80 (CO-CH_2-*CH_2*-S), 42.7 (*CH*-CH_2 main chain PNIPAM), 35.01 (CH-*CH_2*), 41.8 (CO-NH-*CH*-CH_3),: 21.7. (CO-NH-CH-*CH_3*), 174 (*CO*-NH).

IR: $\bar{\nu}$ = 3434, 3288, 3074, 2971, 2933, 2874, 1643, 1542, 1458, 1386, 1366, 1270, 1172, 1130, 1025, 976, 953, 927, 881, 838 cm^{-1}

H5P5 ----------------------

^{1}H NMR (D_2O, 500Hz): 1.0 (CO-NH-CH-*CH_3* PNIPAM), 1.44 (CH-*CH_2* PNIPAM), 1.87 (*CH*-CH_2 main chain PNIPAM), 2.28 (CO-*CH_2*-CH_2-S PNIPAM), 2.37 (N-CH_2-*CH_2*-CO), 2.45 (N-*CH_2*-*CH_2*-N), 2.53 (CO-NH-CH_2-*CH_2*), 2.55 (CO-CH_2-*CH_2*-S PNIPAM), 2.63(N-*CH_2*-CH_2-CO), 3.23 (CO-NH-*CH_2*-CH_2),: 3.75 (CO-NH-*CH*-CH_3 PNIPAM)

^{13}C NMR (D_2O, 500Hz): 53.6 (N-*CH_2*-*CH_2*-N), 51.1 (N-*CH_2*-CH_2-CO), 35.09 (N-CH_2-*CH_2*-CO), 36.51 (CO-NH-*CH_2*-CH_2), 52.0 (CO-NH-CH_2-*CH_2*), 37.05 (CO-*CH_2*-CH_2-S), 27.80 (CO-CH_2-*CH_2*-S), 42.7 (*CH*-CH_2 main chain PNIPAM), 35.01 (CH-*CH_2*), 41.8 (CO-NH-*CH*-CH_3),: 21.7. (CO-NH-CH-*CH_3*), 174 (*CO*-NH).

IR: $\bar{\nu}$ = 3427, 3283, 3076, 2972, 2933, 2875, 1639, 1542, 1458, 1386, 1366, 1274, 1172, 1131, 1023, 953, 928, 882, 839 cm^{-1}

H5P7 ----------------------

^{1}H NMR (D_2O, 500Hz): 1.02 (CO-NH-CH-*CH_3* PNIPAM), 1.45 (CH-*CH_2* PNIPAM), 1.87 (*CH*-CH_2 main chain PNIPAM), 2.27 (CO-*CH_2*-CH_2-S PNIPAM), 2.37 (N-CH_2-*CH_2*-CO), 2.45 (N-*CH_2*-*CH_2*-N), 2.53 (CO-NH-CH_2-*CH_2*), 2.55 (CO-CH_2-*CH_2*-S PNIPAM), 2.63(N-*CH_2*-CH_2-CO), 3.23 (CO-NH-*CH_2*-CH_2),: 3.76 (CO-NH-*CH*-CH_3 PNIPAM)

^{13}C NMR (D_2O, 500Hz): 53.6 (N-*CH_2*-*CH_2*-N), 51.1 (N-*CH_2*-CH_2-CO), 35.09 (N-CH_2-*CH_2*-CO), 36.51 (CO-NH-*CH_2*-CH_2), 52.01 (CO-NH-CH_2-*CH_2*), 37.05 (CO-*CH_2*-CH_2-S), 27.80 (CO-CH_2-*CH_2*-S), 42.71 (*CH*-CH_2 main chain PNIPAM), 35.01 (CH-*CH_2*), 41.8 (CO-NH-*CH*-CH_3),: 21.7. (CO-NH-CH-*CH_3*), 174 (*CO*-NH).

IR: $\bar{\nu}$ = 3434, 3288, 3074, 2971, 2933, 2875, 1641, 1542, 1458, 1386, 1366, 1340, 1273, 1172, 1130, 1024, 953, 927, 882, 839 cm^{-1}

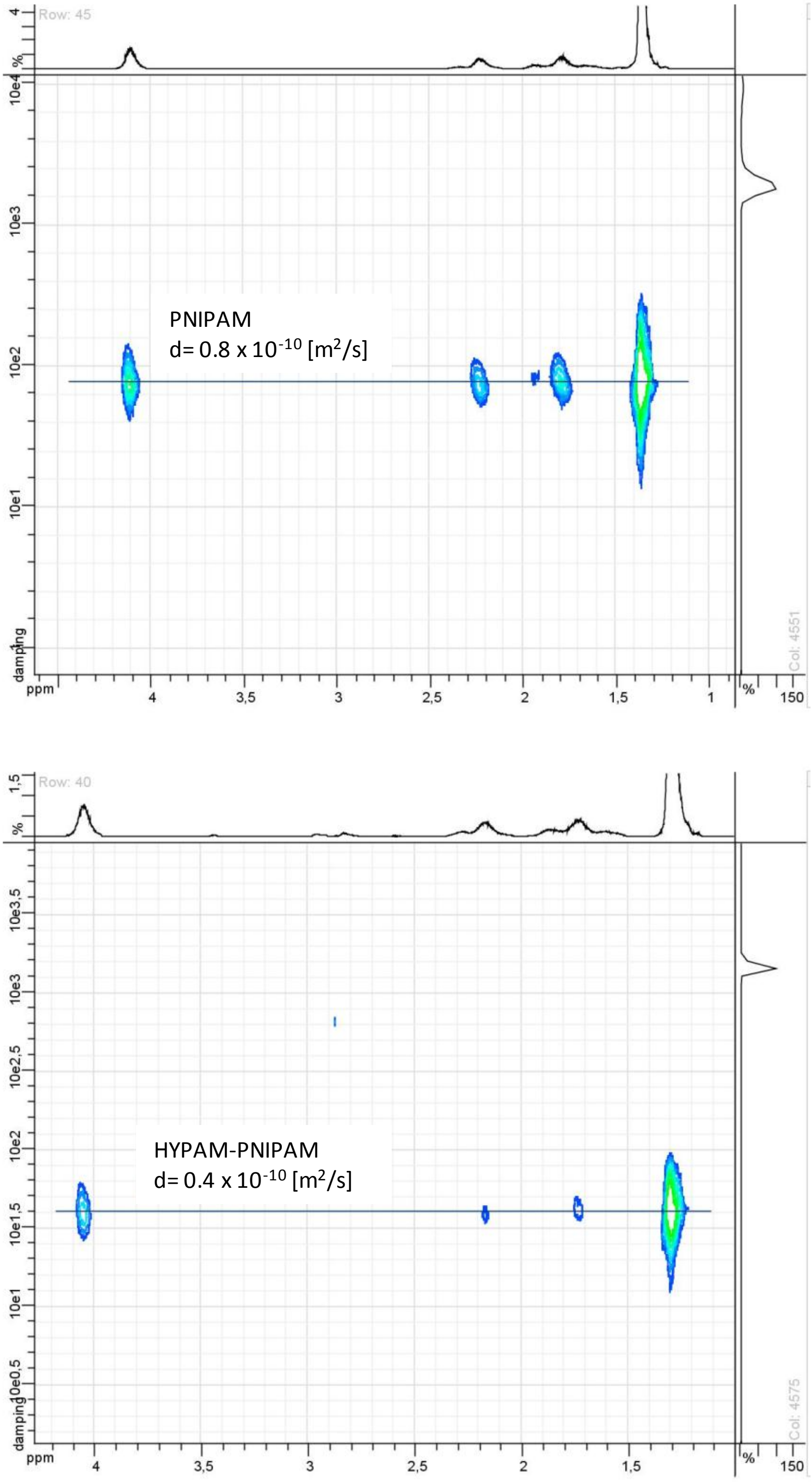

Figure SI 4. PGSE-NMR spectra of P5 and H4P5 in D_2O at 298K and calculated diffusion coefficients.

A.2. Evaluation of grafting ratio

A.2.1: by IR

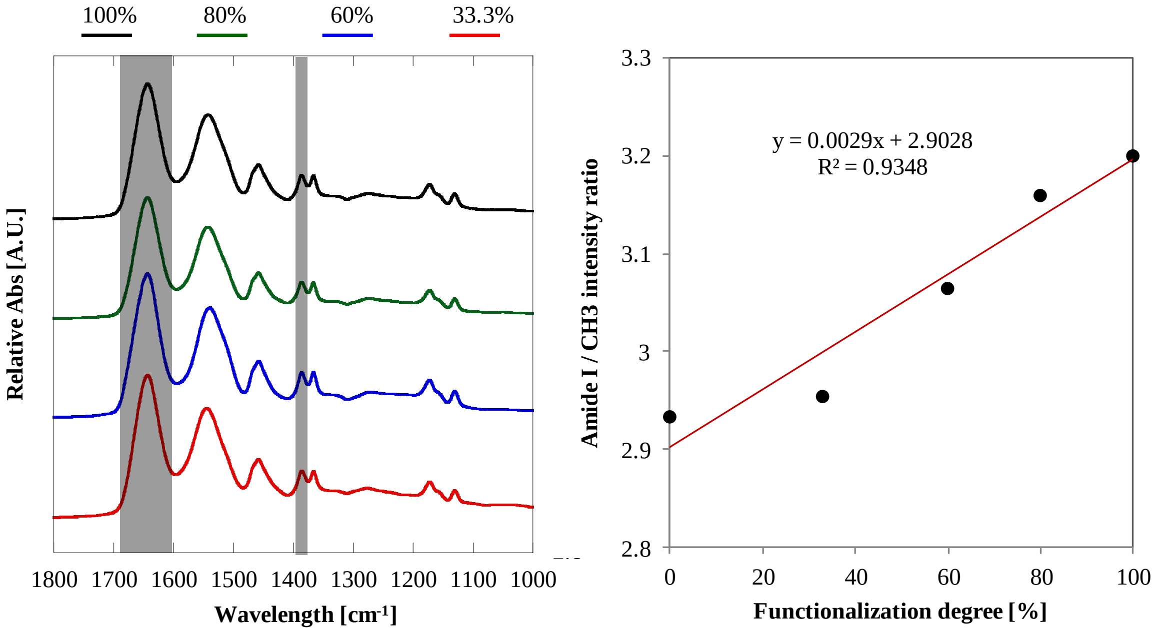

Figure SI 5. On the left: FT-IR spectra of physical mixtures of H4 and P7 corresponding to grafting ratios of 33.3, 60, 80, and 100%. On the right: Corresponding calibration curve giving the ratio between the intensity of amide I band (1641 cm-1) and the one of CH3 deformation band (1386 cm-1) as a function of the grafting ratio.

A.2.2.: by DSC

The grafting ratios were evaluated from DSC experiments using 0.5 wt.% polymer solutions. For this, the variation of enthalpy registered for a given polymer was compared to the variation of enthalpy measured for pure PNIPAM at the same concentration, assuming that grafting does not modify significantly energy involved during the dehydration process. Then PNIPAM weight content in the core shell structures was calculated from the equation below:

$$\text{grafting ratio [\%]} = \frac{\text{wt.}_{P_x}\%}{\left(1-\text{wt.}_{P_x}\%\right)\times n_{NH_2}\times M_{P_x}}\times 100$$

with: $\text{wt.}_{P_x}\%$ = weight content of PNIPAM determined from DSC measurements thanks to the variation of enthalpy, n_{NH_2}[mol.g^{-1}]: amount of primary amines in the core, M_{P_x}: molar weight of PNIPAM.

A.3. Characterization of bulk polymers by DSC

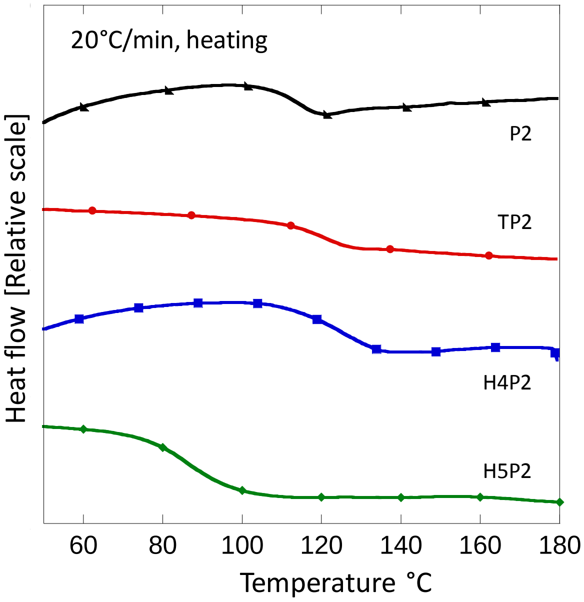

Figure SI 6. DSC thermograms of P2, TP2, H4P2 and H4P2 at a heating rate of 20°C.min^{-1}.

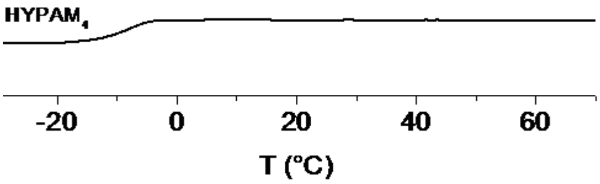

Figure SI 7. DSC thermogram of H4 recorded at a heating rate of 20°C.min^{-1}.

B. Properties of aqueous solutions of hyperbranched polymers

B.1. DSC experiments

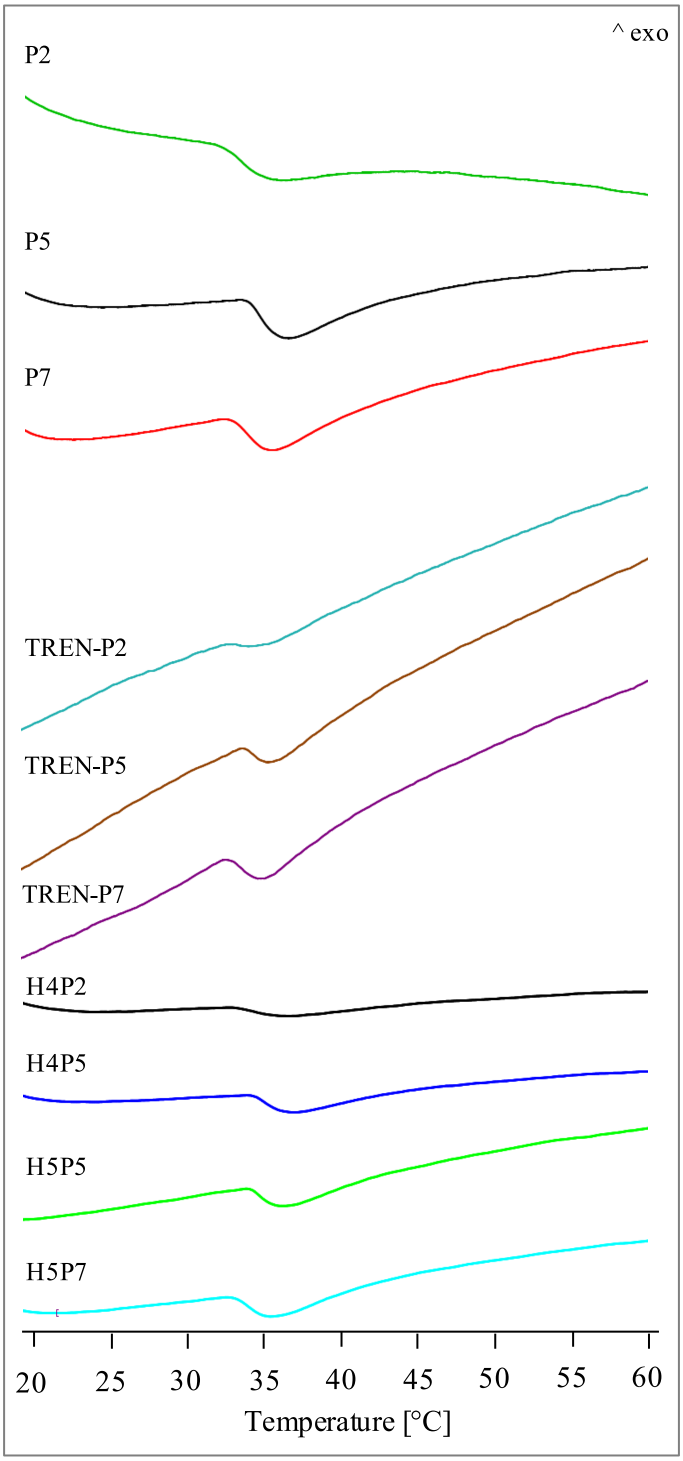

Figure SI 8. DSC thermograms of 0.5 wt. % solutions of PNIPAM and PNIPAM grafted polymers recorded on heating at 1°C.min^{-1}

B.2. TEM images of polymers

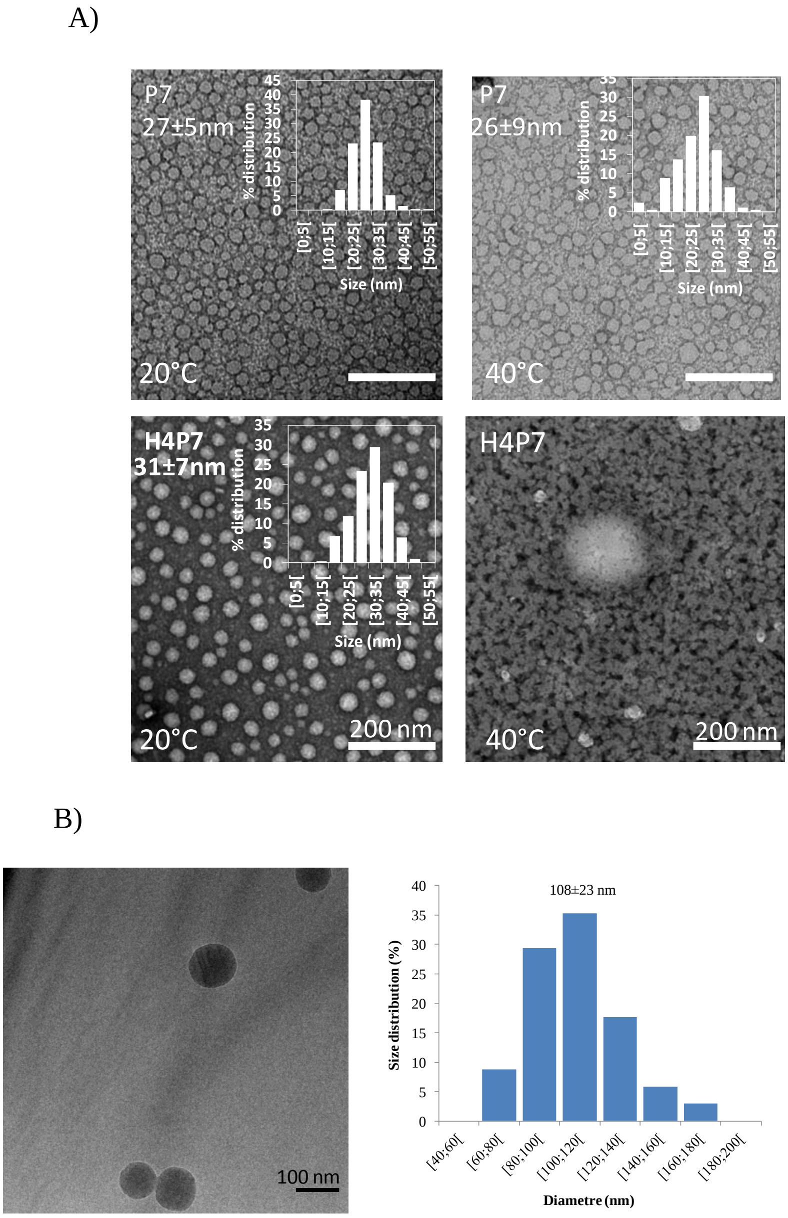

Figure SI 9. A) Representative TEM images of P7 and H4P7 (0.1 wt.% solution samples) stained with uranyl acetate at 20°C and 40°C. B) Cryo-TEM image and corresponding size distribution histogram of polymer H4P7 at 0.5 wt.% in water.

Cryogenic Transmission electron microscopy (CryoTEM). A Jeol 2100 LaB6 microscope was used for the cryo-TEM imaging. 300-mesh lacey carbon-coated copper grids were glow discharged (Leica EM PACT) for 45 s. A 2.5 μL portion of sample solution was applied onto the grids, and the excess of the dispersion was removed by a blotting paper. Liquid ethane cooled to −175 °C was used for sample vitrification. The vitrified sample was cryo-transferred into the cryo-TEM and kept at −180 °C during observation. Micrographs were recorded under low dose conditions (<5 $e^{-}/Å^{2}$) using a Gatan 794 CCD camera operating the microscope in bright field mode, at 100 kV acceleration voltage.

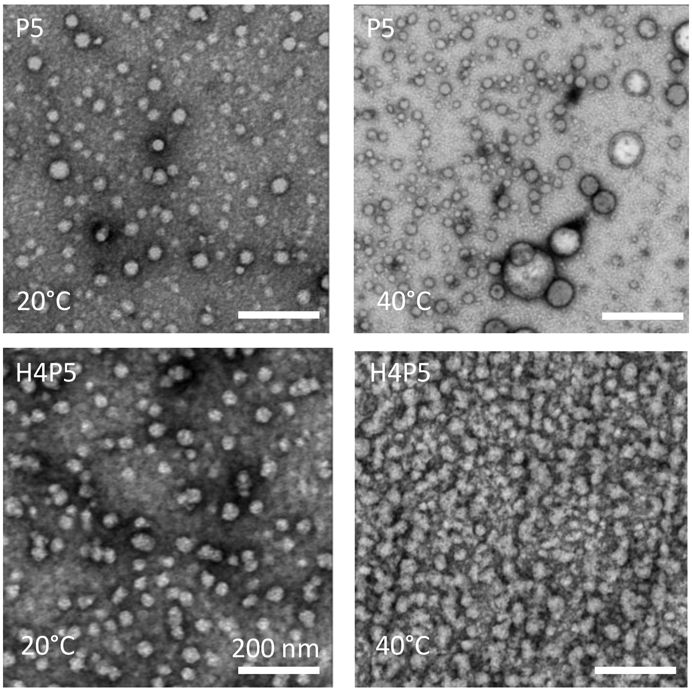

Figure SI 10. Representative TEM images of 0.1 wt.% solutions of P5 and H4P5 stained with uranyl acetate at 20°C and 40°C.

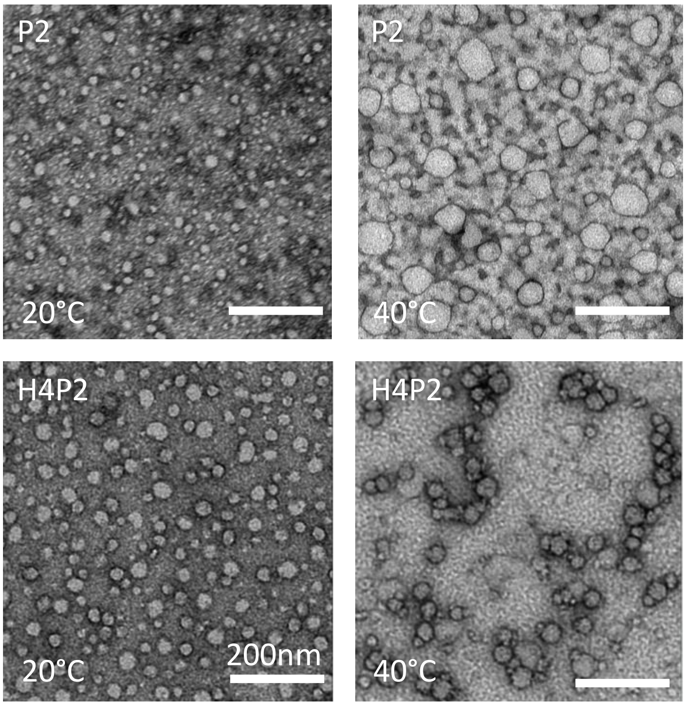

Figure SI 11. Representative TEM images of 0.1 wt.% solutions of P2 and H4P2 stained with uranyl acetate at 20°C and 40°C.

B.3. Temperature-dependent turbidity measurements

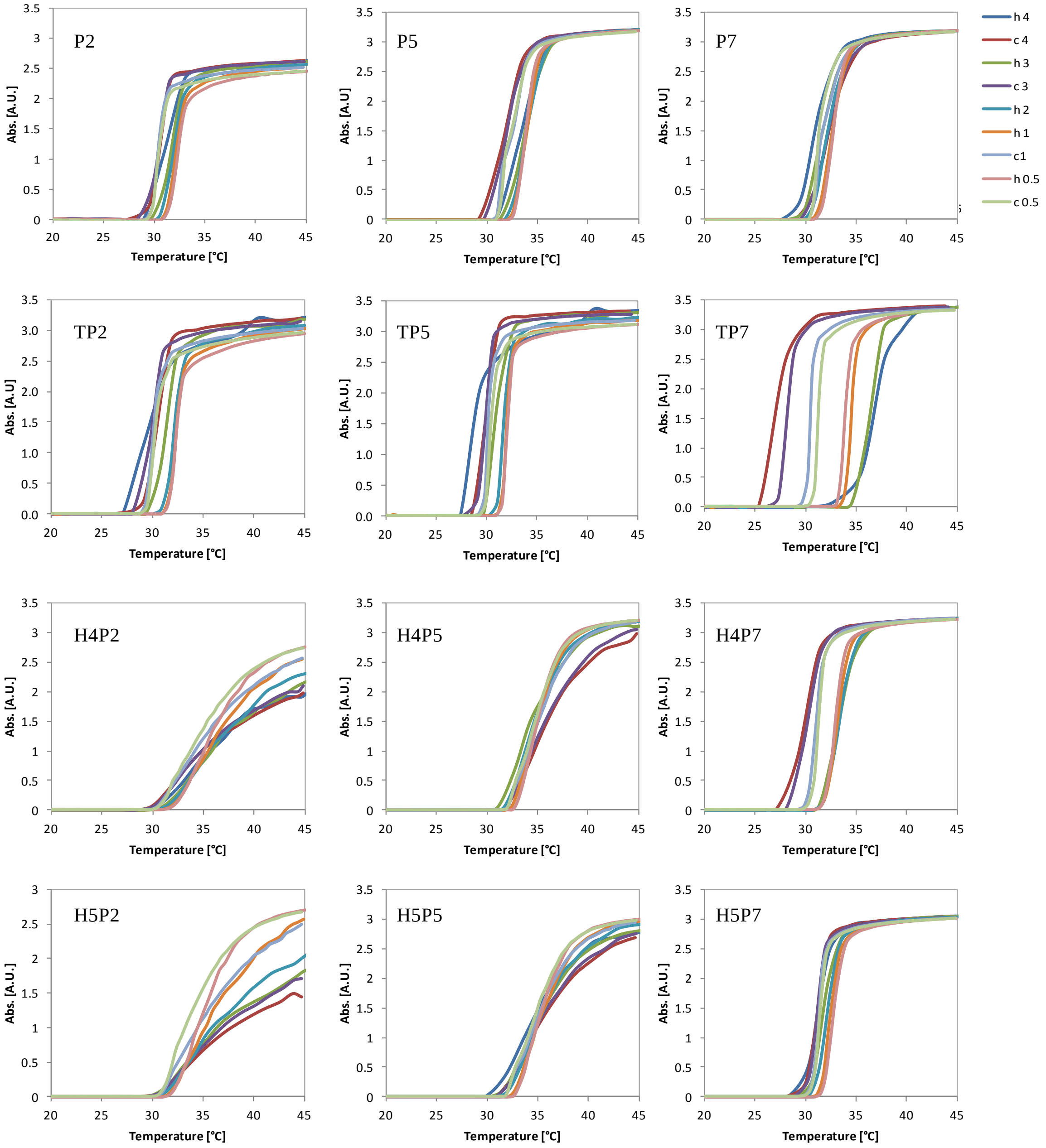

Figure SI 12. Temperature-dependent absorbance at 500 nm for 0.1 wt. % aqueous solutions of PNIPAM and grafted polymers at five heating (h) and cooling (c) rates: 4, 3, 2, 1, 0.5°C.min^{-1} from 20 to 45°C.

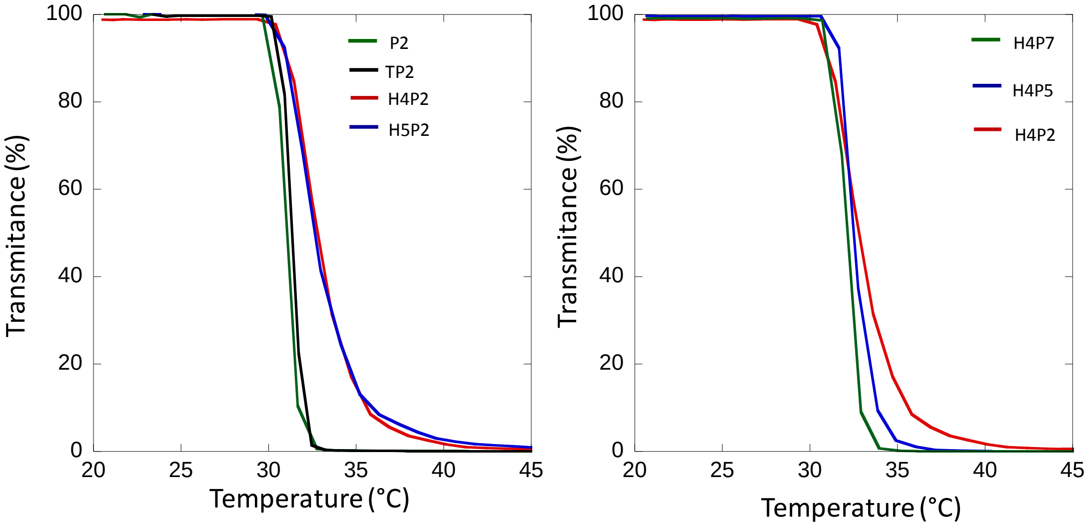

Figure SI 13. Temperature-dependent turbidity at 500 nm for 0.1wt% polymer solutions on heating at 1°C.min^{-1} from 20 to 45°C.

C. PNIPAM based hyberbranched structures as stabilizing agent of gold NPs

C.1. *Ex situ* synthesis and stabilization of AuNPs by PNIPAM based hyperbranched polymers.

C.1.a. Preformed AuNPs

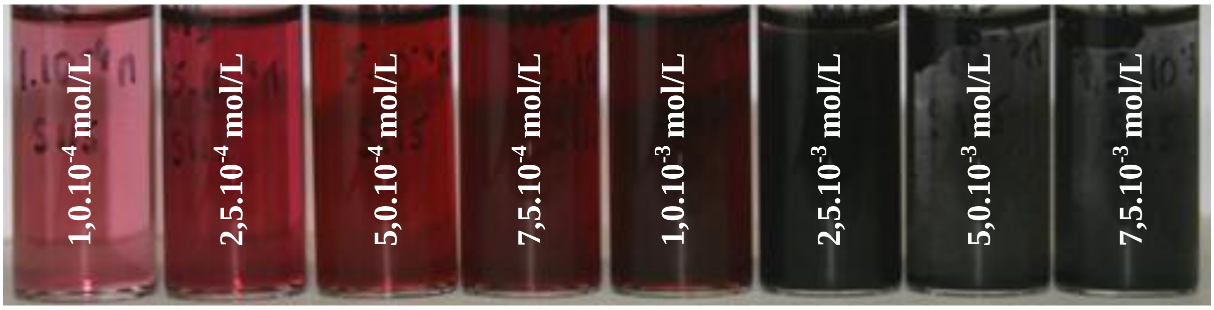

Figure SI 14. Au NPs solutions formed at different $HAuCl_4$ concentrations 10 minutes from the addition of $NaBH_4$ to $HAuCl_4$ ($[HAuCl_4]/[NaBH_4] = 1$).

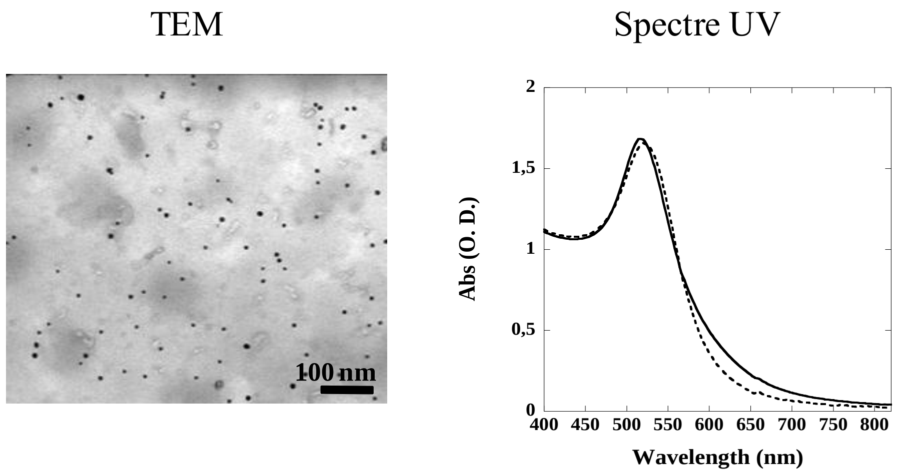

TEM

Spectre UV

Figure SI 15. TEM image (left) and UV-vis spectra (right) of colloidal dispersions of AuNPs (diameter equal to 5±1 nm) synthesized by reduction of $HAuCl_4$ (5×10^{-4} mol·L^{-1}) with one equivalent of $NaBH_4$ obtained after 1 hour (solid line) and 1 month (dash line).

C.1.b. Stabilization of AuNPs in presence of PNIPAM based hyperbranched polymers

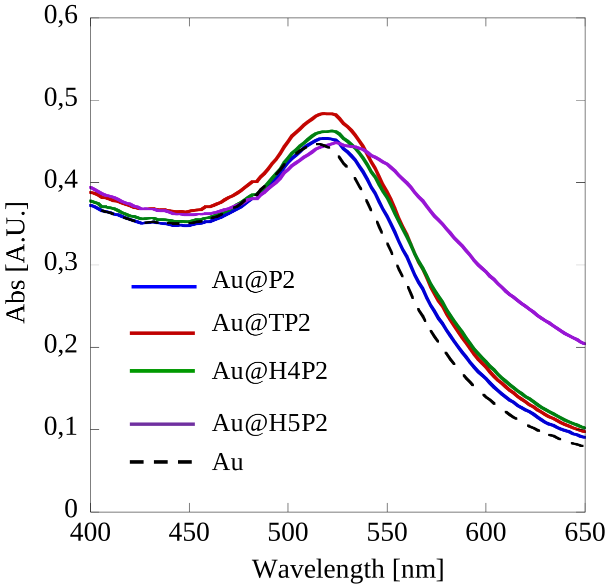

Figure SI 16. UV Spectra of colloid solutions of polymer-coated AuNPs (solid line) and AuNPs without polymer (dash line). [AuNPs]=2.5×10^{-4} mol·L^{-1} and [polymer]=0.05 wt.%.

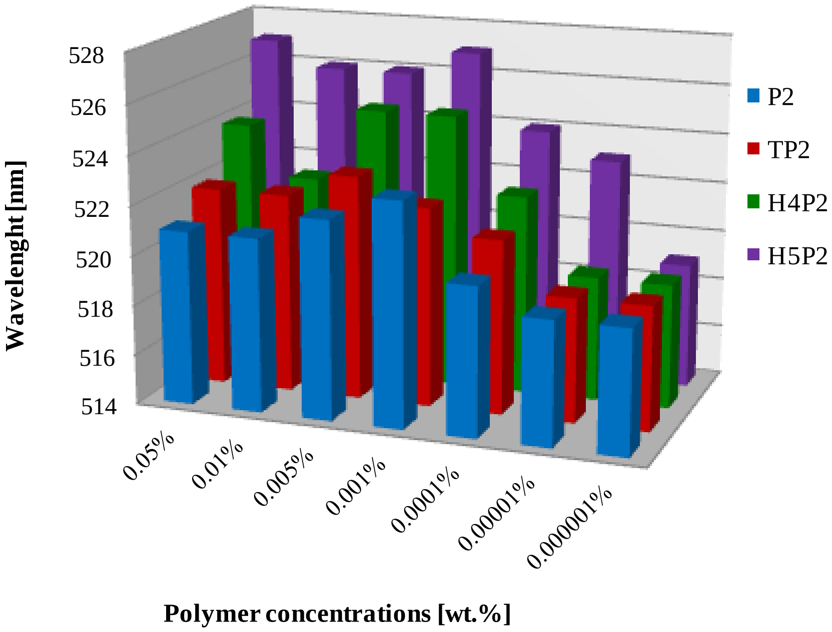

Figure SI 17. λ_{max} values obtained from absorbance spectra for preformed AuNps coated with P2, TP2, H4P2 and H5P2 ([AuNPs]=2.5×10^{-4} mol·L^{-1} and [polymer]=0.05 wt.%. to 10^{-6} wt.%).

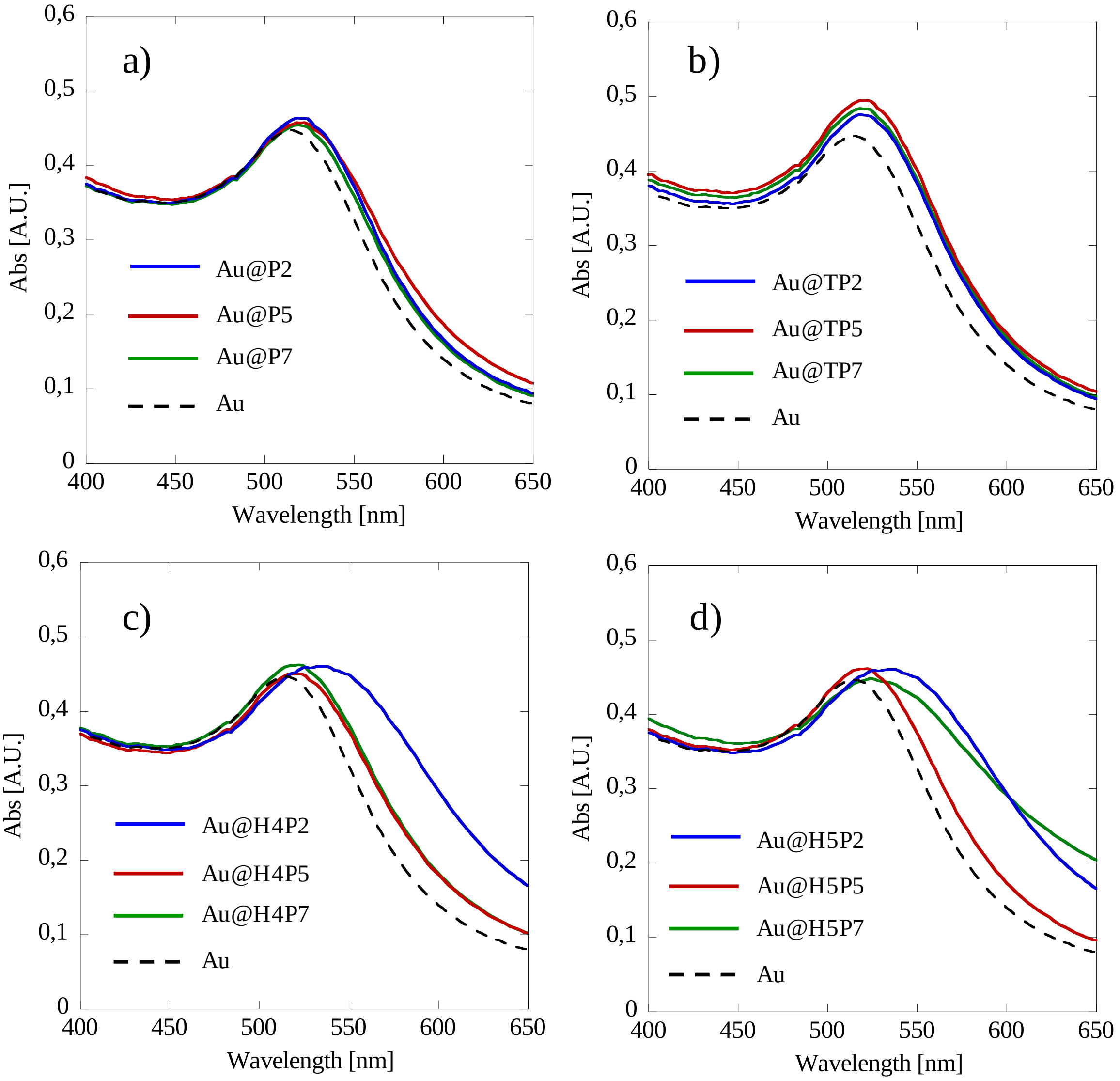

Figure SI 18. UV Spectra of colloid solutions of polymer-coated AuNPs (solid line) a) Au@Px, b) Au@TPx, c) Au@H4Px, d) H5Px@Au; and AuNPs without polymer (dash line). [AuNPs]=2.5×10^{-4} mol·L^{-1} and [polymer]=0.05 wt.%.

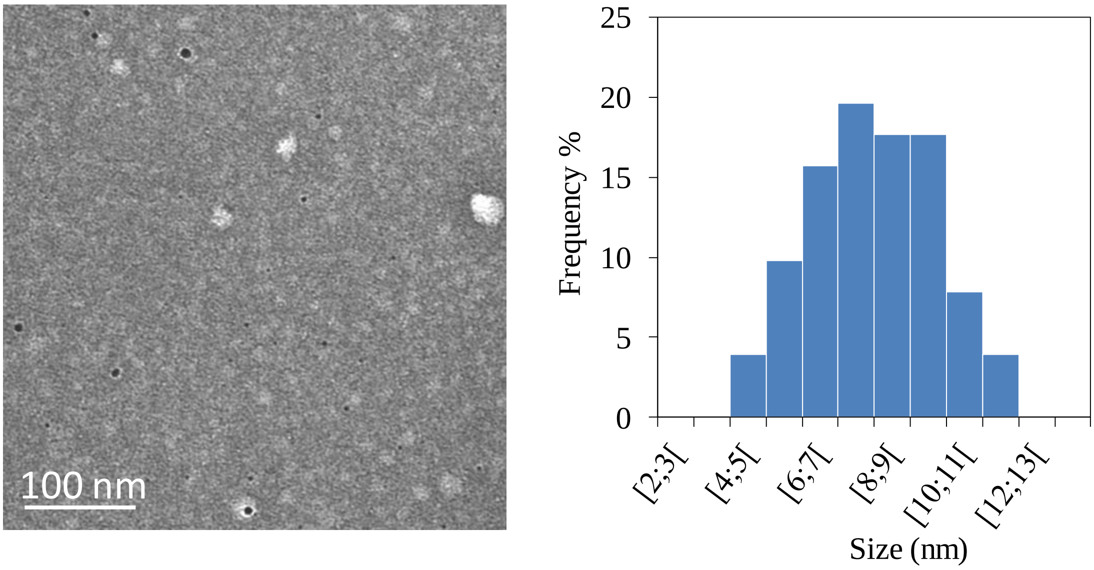

Figure SI 19. TEM image and corresponding size histogram of H4P5@Au colloid solution. [AuNPs]= 2.5×10^{-4} mol·L^{-1} and [polymer]= 0. 1 wt.%.

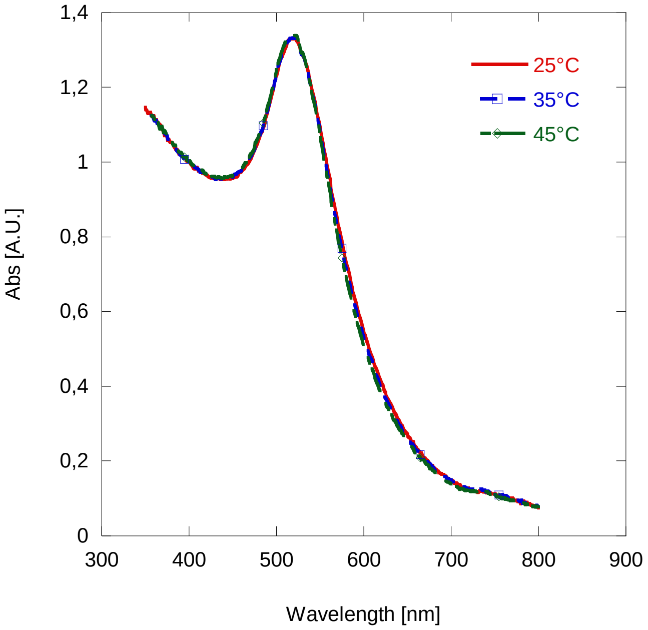

Figure SI 20. Evolution of absorption spectra of AuNPs colloid solution (without polymer coating) with increasing temperature. [AuNPs]= 2.5×10^{-4} mol·L^{-1} and [polymer]= 0 wt.%.

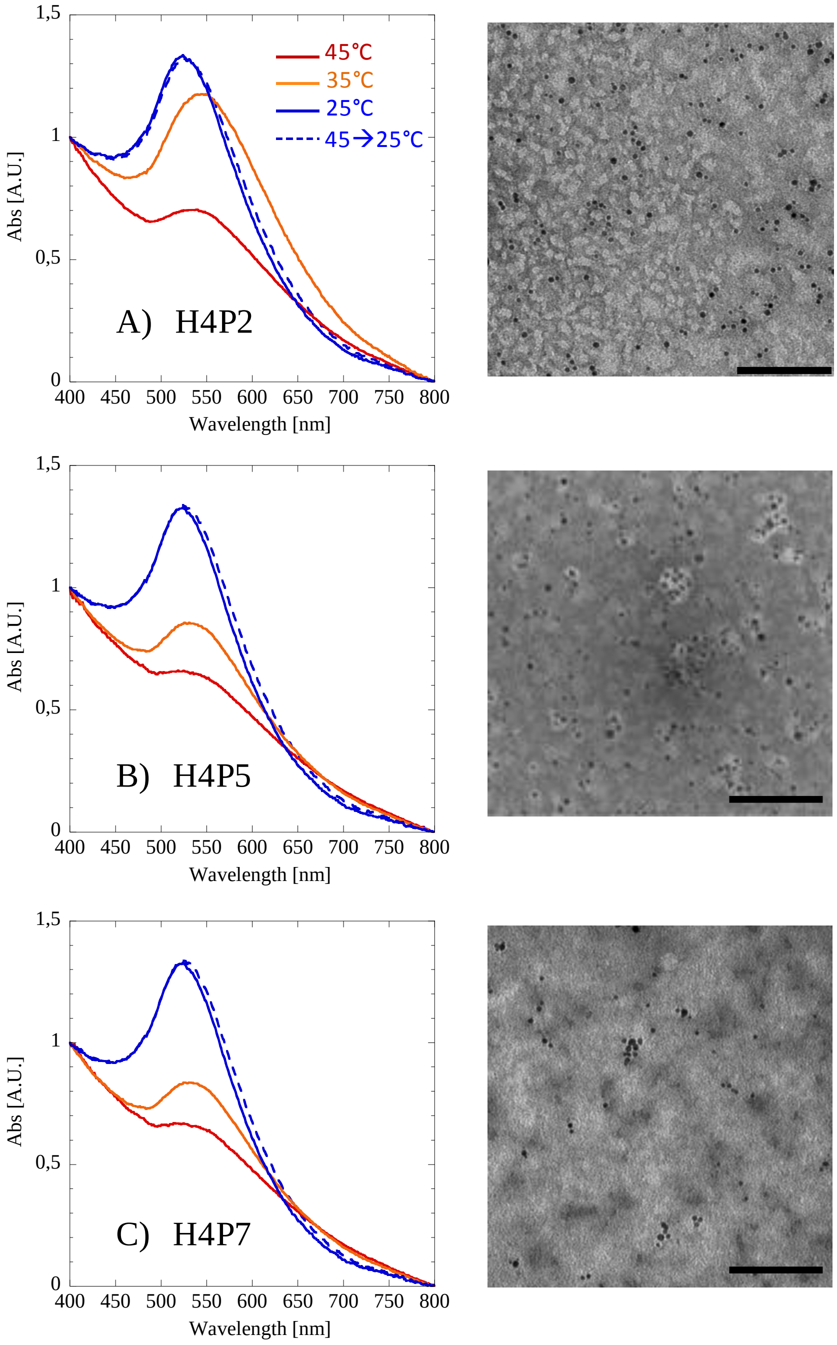

Figure SI 21. Changes in absorption spectra of Au@H4P2, Au@H4P5 and Au@H4P7 with increasing temperature and corresponding TEM images. The absorbance at 800 nm was subtracted from the spectra, then normalized at 400 nm to remove scattering contribution and multiplied by a factor in a way that absorbance vary from 0 to 1. [AuNPs]=2.5×10^{-4} mol·L^{-1} and [polymer]=0.05 wt.%.

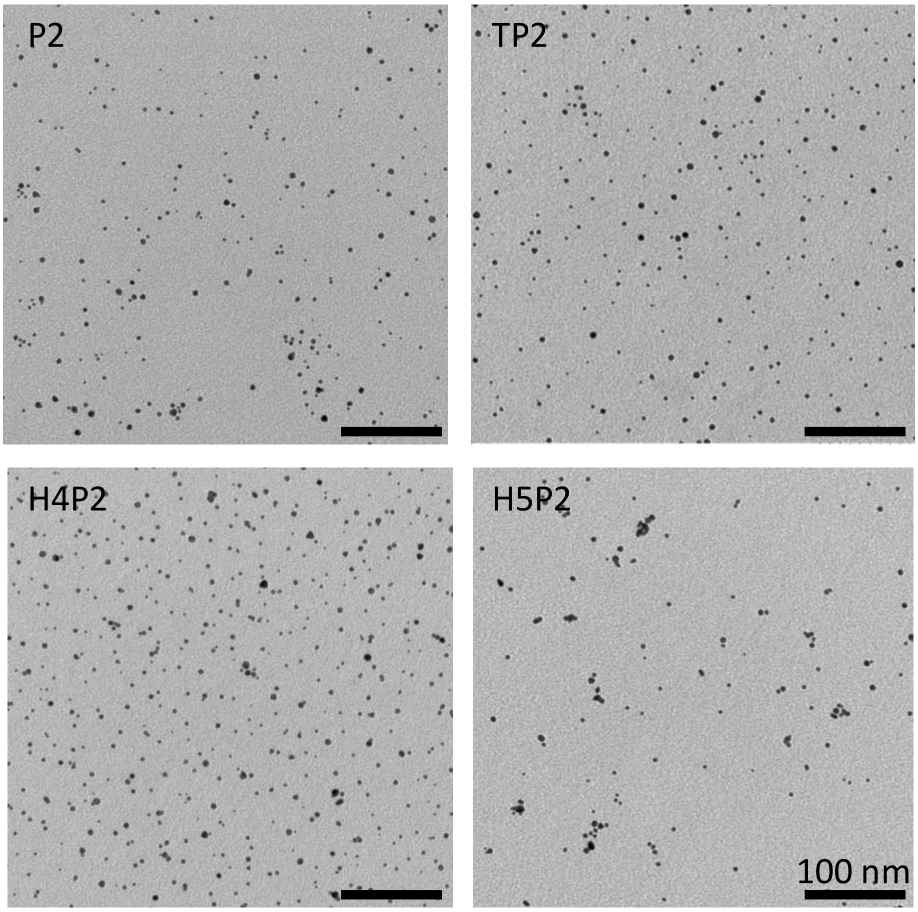

Figure SI 22. TEM images of polymer-coated AuNPs deposited at 25°C. [AuNPs]= 2.5×10^{-4} $mol\cdot L^{-1}$ and [polymer]= 0.05 wt.%

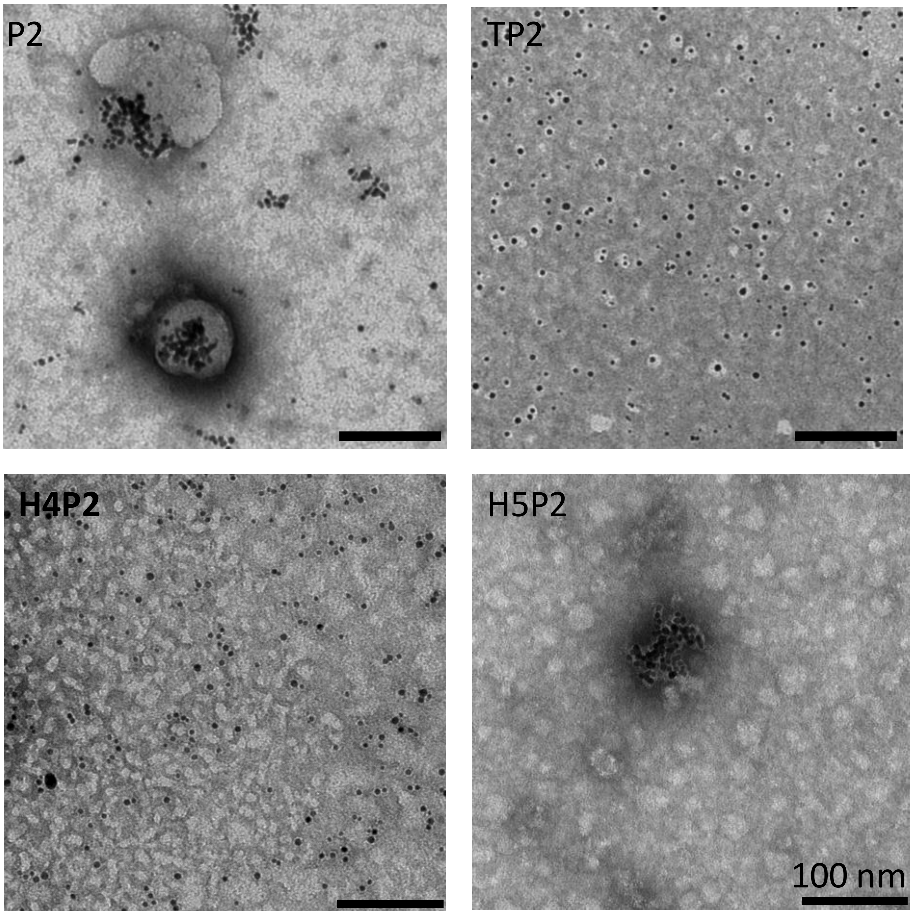

Figure SI 23. TEM images of polymer-coated AuNPs deposited at 45°C. [AuNPs]= 2.5×10^{-4} mol·L^{-1} and [polymer]= 0.05 wt.%

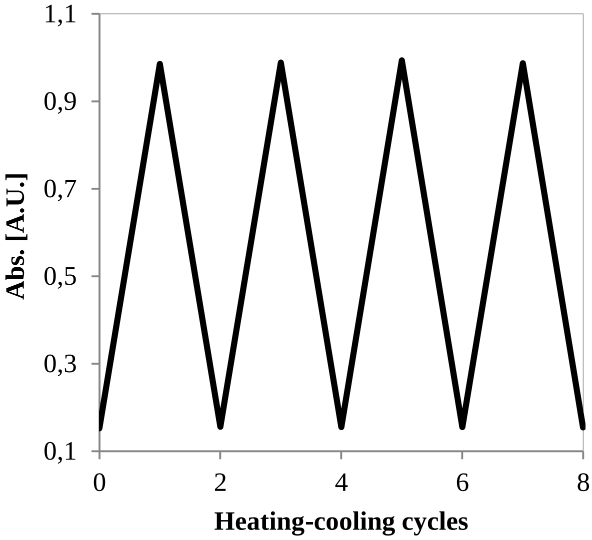

Figure SI 24. Relative absorbance at 650 nm in function of heating-cooling cycles between 25 to 45 °C for Au@H4P7 colloid solution. [AuNPs]=2.5×10^{-4} mol·L^{-1} and [polymer]=0.05 wt.%.

C.2. *In-situ* synthesis of AuNPs

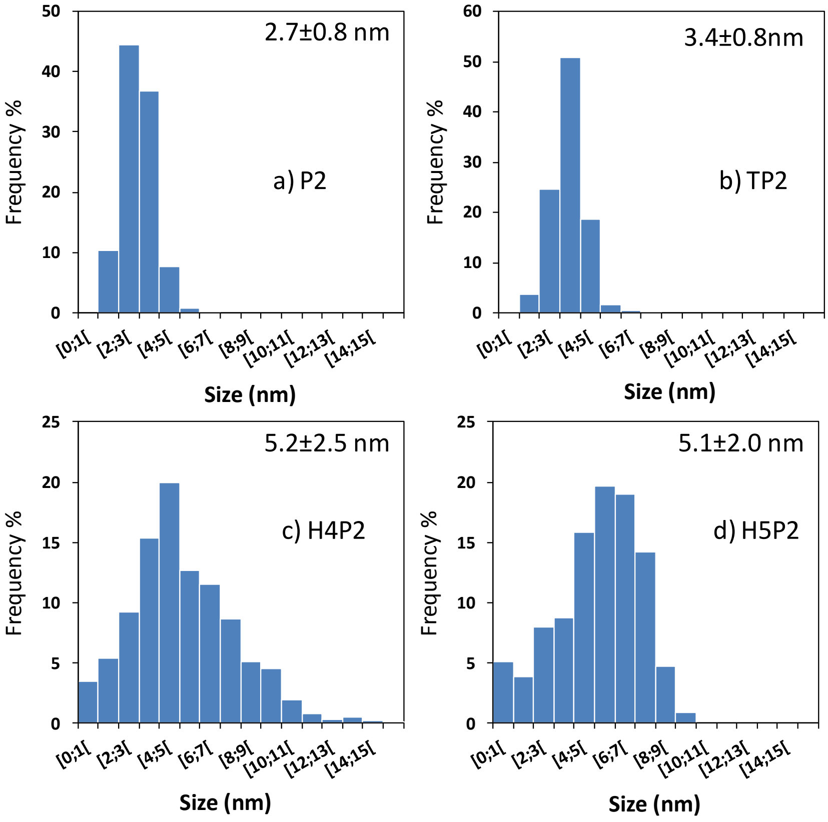

Figure SI 25. Histogram of diameter distribution for *in situ* synthesized AuNPs in polymer solution, final [AuNPs]= 2.5×10^{-4} mol·L^{-1} and [polymer]= 0.01 wt.%

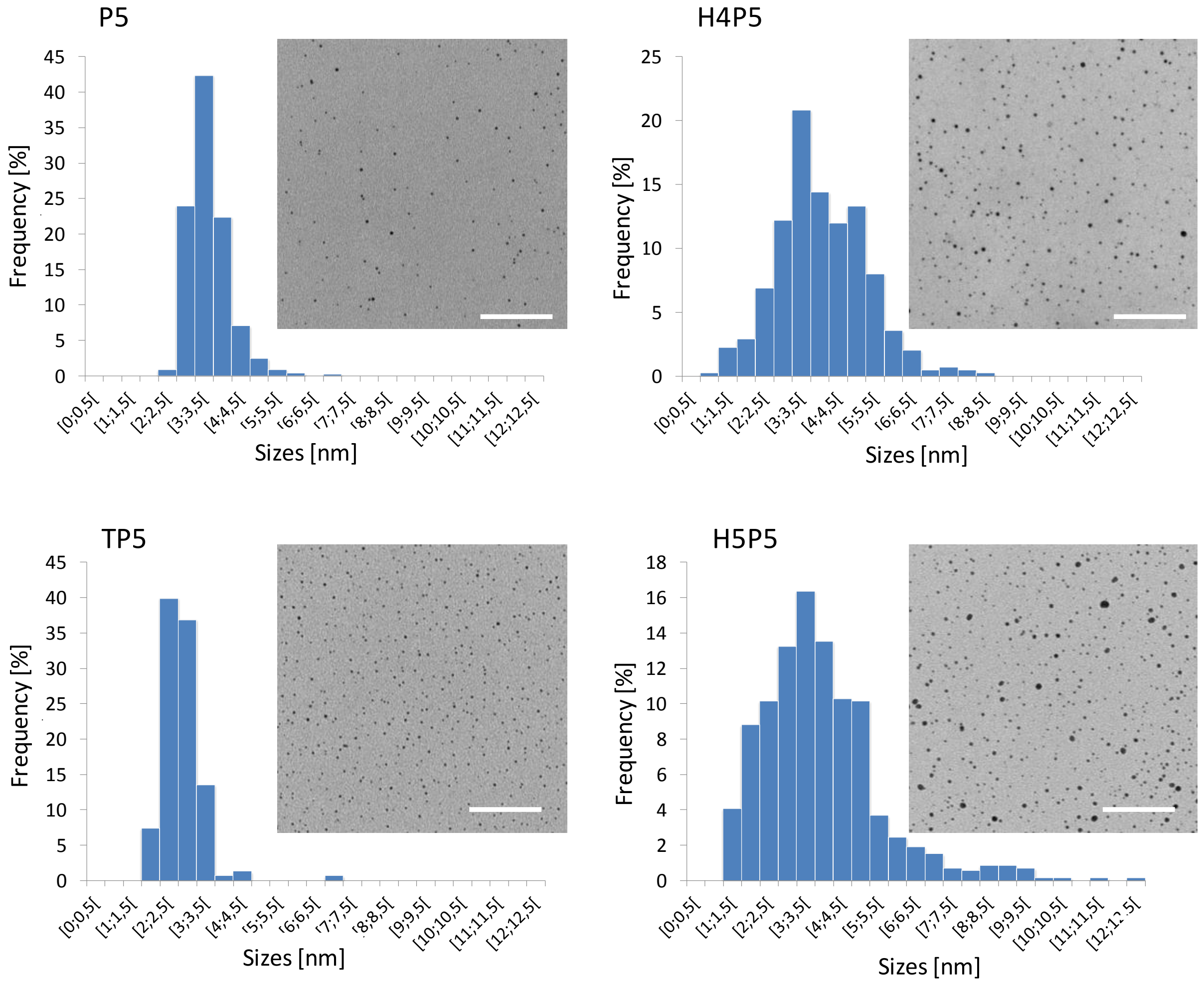

Figure SI 26. TEM images and corresponding diameter distribution of *in situ* synthesized AuNPs in polymer solution, final [AuNPs]= 2.5×10^{-4} mol·L^{-1} and [polymer]= 0.01 wt.%. Scale bar: 100 nm

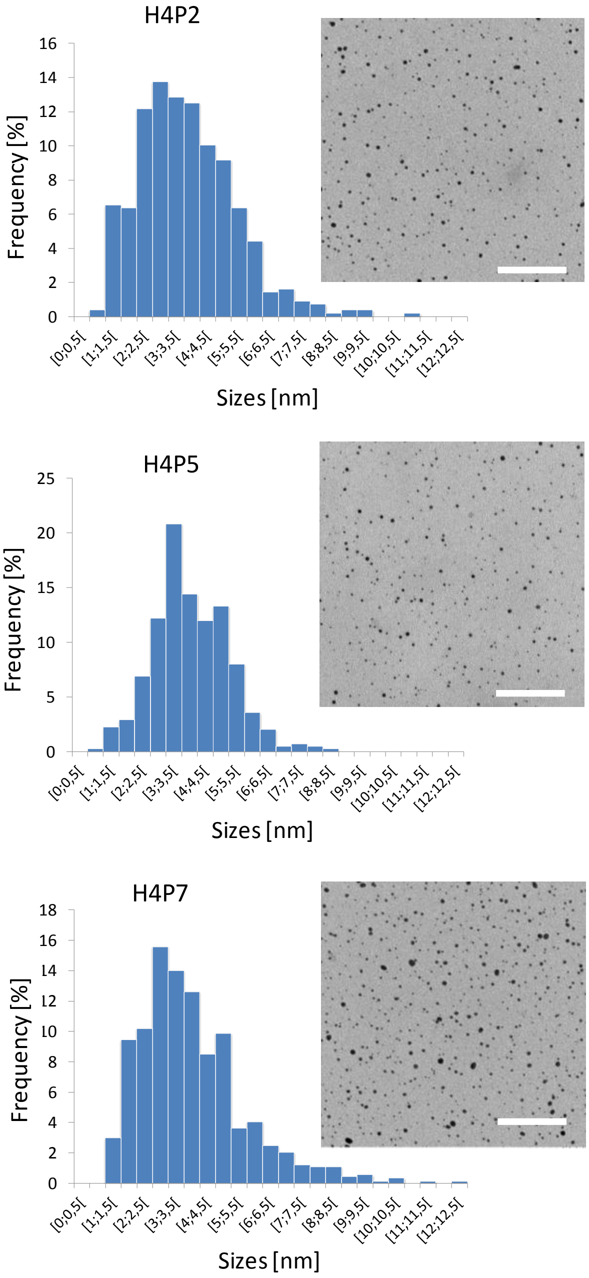

Figure SI 27. TEM images and corresponding diameter distribution of *in situ* synthesized AuNPs in polymer solution, final [AuNPs]= 2.5×10^{-4} mol·L^{-1} and [polymer]= 0.01 wt.%. Scale bar: 100 nm

Table SI 1. Diameter (nm) of *in situ* synthesized AuNPs in polymer solution, final [AuNPs]= 2.5×10^{-4} mol·L^{-1} and [polymer]= 0.01 wt.%

Shell\core	Ø	TREN	H4	H5
P2	2.7±0.8	3.4±0.8	5.2±2.5	5.1±2.0
P5	3.1±0.8	3.2±0.7	5.0±2.0	3.5±1.5
P7	3.8±1.2	3.3±1.9	4.4±2.3	3.5±1.7

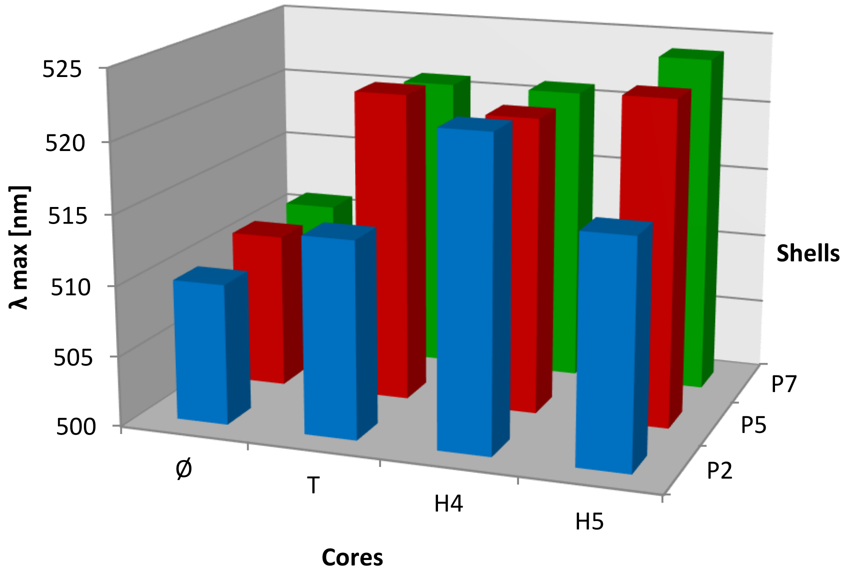

Figure SI 28. λ_{max} value obtained from UV spectra for polymer-coated AuNps, [AuNPs]= 2.5×10^{-4} mol·L^{-1} and [polymer]= 0.01 wt.%

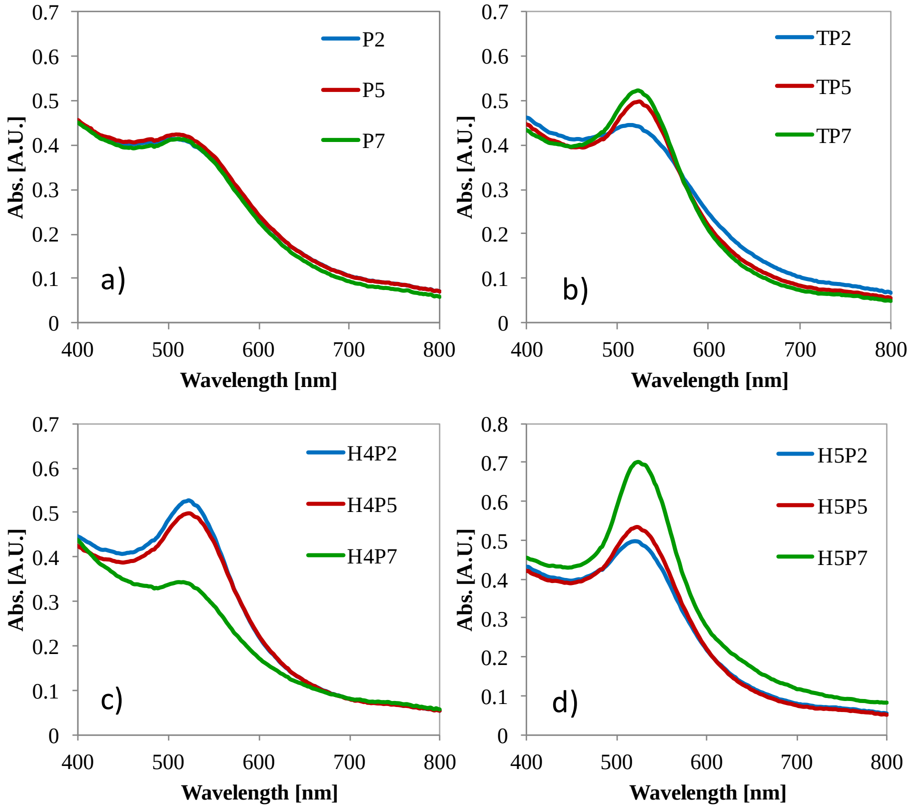

Figure SI 29. Absorbance spectra of *in situ* synthesized AuNps in polymer solution a) Px, b) TPx, c) H4Px, d) H5Px, x= 2, 5 or 7. [AuNPs]= 2.5×10^{-4} mol·L^{-1} and [polymer]= 0.01 wt.%

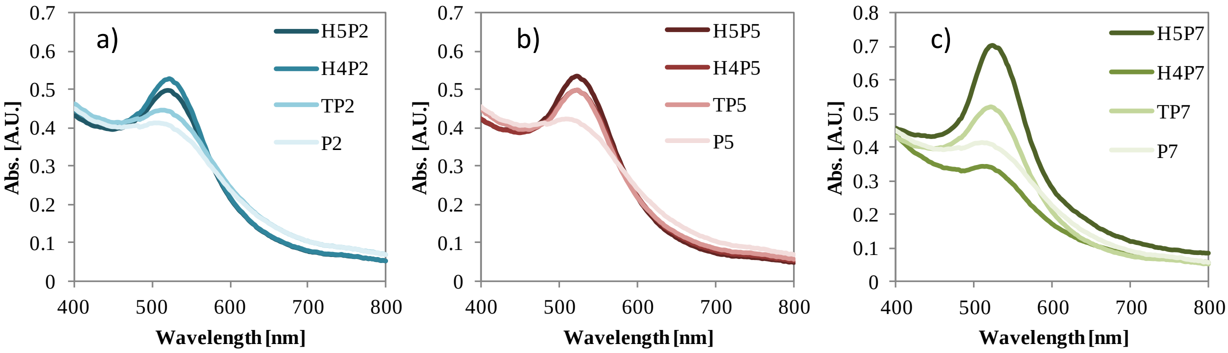

Figure SI 30. Absorbance spectra of *in situ* synthesized AuNPs in polymer solution a) P2 and P2 grafted polymers, b) P5 and P5 grafted polymers, c) P7 and P7 grafted polymers. [AuNPs]= 2.5×10^{-4} mol·L^{-1} and [polymer]= 0.01 wt.%